Research Paper
Computational Methods for Differential Equations
http://cmde.tabrizu.ac.ir
Vol. *, No. *, *, pp. 1-17
DOI:10.22034/cmde.2024.58656.2482

SEI_aI_sQRS epidemic model for COVID-19 by using compartmental analysis and numerical simulation

Hossein Gholami Chahkand[1], **Mortaza Gachpazan**[1], **and Majid Erfanian**[2,*]
[1]Department of Applied Mathematics, School of Mathematical Sciences, Ferdowsi University of Mashhad, Mashhad, Iran.
[2]Department of Science, School of Mathematical Sciences, University of Zabol, Zabol, Iran.

Abstract

In this paper, we developed a SEI_aI_sQRS epidemic model for COVID-19 by using compartmental analysis. In this article, the dynamics of COVID-19 are divided into six compartments: susceptible, exposed, asymptomatically infected, symptomatically infected, quarantined, and recovered. The positivity and boundedness of the solutions have been proven. We calculated the basic reproduction number for our model and found both disease-free and endemic equilibria. It is shown that the disease-free equilibrium is globally asymptotically stable. We explained under what conditions, the endemic equilibrium point is locally asymptotically stable. Additionally, the center manifold theorem is applied to examine whether our model undergoes a backward bifurcation at $\mathcal{R}_0 = 1$ or not. To finish, we have confirmed our theoretical results by numerical simulation.

Keywords. Backward bifurcation, Globally asymptotically stable, Basic reproduction number.
2010 Mathematics Subject Classification. 65L60; 44A45; 45B05; 65R20.

1. Introduction

Diseases have always played an important role in human history. Infectious diseases have had a significant impact on population growth, victory in wars, and the country's economy. A famous example of the impact that a disease may have on societies is the plague of the 14th century, which is known as the black death. This disease began in Europe around 1346 AD. It is estimated that from that time to 1350, about 20 million people died due to the plague [7]. Another important example is the outbreak of smallpox between 1507 and 1900 in America. A sudden outbreak of the disease began in 1517 and killed about a third of the native population of the island of Hispaniola [18]. In 1520 the disease reached Mexico and it is believed that half of the population of Mexico was killed. Until 1798, when the smallpox vaccine was developed by Edward Jenner, thousands of people lost their lives due to this disease [6]. Currently, the human immunodeficiency virus (HIV), which is the cause of acquired immunodeficiency syndrome (AIDS) in humans, strongly affects the mortality pattern in developed and developing countries. Sub-Saharan Africa, where there were about 23.6 million people with HIV by the end of 2004, has been most affected by this disease [2]. Also, severe acute respiratory syndrome (SARS) started in China in November 2002 and from February 2003 to August 2003, when it was brought under control, it caused 623 deaths in 30 countries [31]. In December 2019, an outbreak of a viral disease was reported in the Chinese city of Wuhan. The cause of this disease was a new type of genetically modified virus from the family of coronaviruses called SARS-CoV-2, which was named the disease of COVID-19 [36]. Unfortunately, due to its high contagiousness, this virus quickly expanded throughout the world and infected all the countries of the world in a short period (less than four months) [32, 35]. This virus and the COVID-19 disease that spreads through it have affected global health and healthcare systems in countries and continents. Considering the global prevalence and the complexity of the characteristics of the disease of COVID-19, a deeper investigation of this virus and the characteristics of the disease seems necessary.

Received: 29 September 2023 ; Accepted: 03 August 2024.
∗ Corresponding author. Email: erfaniyan@uoz.ac.ir.

The mentioned cases show well the impact that disease can have on the population of society and emphasize the need to study how the disease spreads as a branch of science called epidemiology. Epidemiology is the science of studying the spread of diseases to find out the factors involved in their occurrence.
Fever, fatigue, and dry cough are the most common symptoms of COVID-19. Some patients may have other symptoms such as pain and bruising, nasal congestion, runny nose, sore throat, or diarrhea. These symptoms are usually mild and their onset is gradual. Some affected people may not experience any of the symptoms of the disease and feel unwell. Almost out of every 6 people infected with COVID-19, one person becomes seriously ill and suffers from shortness of breath. This disease can spread to others through droplets that are spread around by coughing or exhaling from the mouth and nose of a person infected with COVID-19. These droplets are spread on the devices and surfaces around the sick person. Then, other people get infected with COVID-19 by touching these equipment or contaminated surfaces and touching their eyes, mouth, and nose. It is also possible to get infected by breathing in droplets from the cough or exhalation of a person infected with COVID-19. For this reason, it is important to keep a distance of at least one meter from the person infected with COVID-19.
Despite the existence of extensive preventive and therapeutic measures, such as improving the level of public health, antibiotics, and vaccination, infectious diseases are still the most important cause of death caused by the disease.
The role of quarantine as a preventive strategy in preventing the spread of COVID-19 disease is very important in society and public health. Quarantine measures by limiting social contacts, travel arrangements, and physical restrictions have significant effects in reducing the rate of disease spread. These measures allow society and health systems to use the time to acquire data, run tests, track and trace suspicious cases, and create health facilities to optimally control and prevent the spread of this disease.
The spread of infectious diseases and how to control them has been a significant issue in recent years, and mathematical models are an important tool for investigating this issue. Mathematical models have the potential to predict the course of the disease and estimate the rate of disease transmission, the rate of death, and the recovery of patients. Currently, the purpose of applying mathematical models is to investigate the impact of the COVID-19 disease on the population, the measures required by public health institutions, and the effectiveness of various quarantine measures. Recently, various models, both simple and complex, which include various parameters and variables, have been used to achieve this goal. Also, mathematical and numerical analysis in the study of COVID-19 play a very important role in explaining and predicting the spread of the disease, the impact of various interventions, and optimizing control strategies. From simple mathematical models to more complex models based on dynamic analysis methods, temporal analysis, and complex networks, these methods allow researchers and decision-makers to gain a better understanding of disease behavior and the impact of various interventions. In recent decades, many authors and researchers have discussed and analyzed mathematical models for predicting and controlling epidemics in their articles [1, 3, 13, 16, 17]. Neil F. Johnson is one of the prominent researchers who analyze mathematical epidemic models in his articles. He pays attention to the effect of the spread of networks on the spread of diseases and the complications related to them and uses modeling methods [21, 23]. Also, Alison Galvani is one of the researchers who deals with mathematical epidemic models and analyzes and predicts the spread of diseases using mathematical models in her articles [12, 26].
The spread of infectious diseases and their effects on society and health systems require a more accurate understanding of patterns of spread and prediction of temporal changes. In this regard, the use of dynamic models as a powerful and efficient tool in the analysis and prediction of infectious diseases has been considered. Dynamic models show the changes and interactions between different factors of infectious diseases by using mathematical equations and time information. These models can simulate and predict disease behavior in different societies and responses to different variables. Due to the complexity and discontinuity of the factors affecting the spread of infectious diseases, dynamic models provide the possibility of analyzing the effects of various variables including population, prevalence, vaccination, people's behavior, and health interventions. In this type of model, the population is divided into several parts, assuming that all the people in one part of the population have the same behavior. For example, Akuka et al in [4] designed a susceptible (S), individuals who have received the first dose of vaccine (V_1), individuals who have received the second dose of vaccine (V_2), exposed (E), quarantined (Q), infected (I) and recovered (R) model. By using numerical experiments, they concluded intervention measures such as double-dose vaccination and quarantine help to reduce the spread of COVID-19. Teklu in [34] used a susceptible (S), protected (P), vaccinated (V), infected (I),

hospital quarantined (Q_1) and home quarantined (Q_2) model. He concluded that the protective measures outlined in his paper will help reduce the spread of the COVID-19 disease. In addition, Ghostin et al. in [19] proposed a susceptible (S), exposed (E), infectious (I), quarantined (Q), recovered (R), deaths (D), and vaccinated (V) model to simulate the novel coronavirus disease spread in Saudi Arabia. They used the Kalman filter to constrain the model outputs and its parameters with available data. Das et al in [14] introduced a susceptible (S), asymptomatically infected (I_a), symptomatically infected (I_s), hospitalised (H) and recovered (R) dynamical model. They showed that public behavior and government measures, for example, social distancing, vaccination, and awareness programs are more useful than only public responses to minimize the spread of COVID-19 pandemic. Algarni et al in [5] studied a susceptible (S), vaccinated (V), symptomatically infected (I), asymptomatically infected (A) and recovered (R) dynamical model. They showed that the vaccine reduces the transmission rate. Their work explains the rise in the number of new infectious immediately after the start of the vaccination campaign in Saudi Arabia. Hail et al in [20] considered a susceptible (S), latent infected (L), undetected infected (I_u), detected infected (I_d), recovered (R) dynamical model. They attempted to estimate the mean proportion of correctly confined sub-populations in Morocco as well as its effect on the continuing spread of COVID-19. A fitting to Moroccan data is established. In addition, interested readers can refer to [27–30] and the references therein.

Several researchers have used fractional derivatives to analyze diseases and physical phenomena. For example, Rezapour et al. [33] presented a model for COVID-19 using the Caputo fractional derivative. Based on Real data, they introduced a numerical simulation to forecast the transmission of disease in Iran and in the world. Baishya et al [8] concentrated on the examination of the Bloch equation affected by the Caputo fractional derivative, both with and without delay, and explores the underlying chaos utilizing a sliding mode controller. Mohammadaliee et al. [25] introduced a model for COVID-19 using the ψ-Caputo fractional derivative. They have showed that when the order of derivative is equal to 0.95 then, the prevalence of the disease is better. Kherraz et al [24] studied boundary value problems for fractional differential equations with multiple orders of fractional derivative and integrals. Houas and Samei [22] examined the Duffing-Rayleigh type problem with sequential fractional q-derivative of the Caputo type.

In this paper, we introduce and analyze an SEI_aI_sQRS epidemic model which includes a quarantine program that helps to limit COVID-19.

This paper is organized as follows: in section 2, the proposed model is formulated. The positivity and boundedness of solutions are proved in this section. In section 3, the equilibrium points and basic reproduction number for the model are obtained. In section 4, we present stability analysis for the equilibrium points. Section 5 is dedicated to backward bifurcation analysis. Sensitivity analysis and numerical experiments are discussed in section 6 and finally conclusion is in section 7.

2. Model formulation

This new model will be divided into some compartments such as the total human population size at time t, denoted by N(t) and it comprises of the susceptible (S), exposed (E), symptomatically infected (I_s), asymptomatically infected (I_a), quarantined (Q), and recovered (R) compartments.

2.1. **Formulation of the model.**

If we denote the total population by N, then we have

$$N(t) = S(t) + E(t) + I_a(t) + I_s(t) + Q(t) + R(t). \tag{2.1}$$

The model variables and parameters are introduced in Table 1. The model is mathematically formulated as a system of ordinary differential equations :

$$\begin{aligned}
\frac{dS}{dt} &= \Lambda + \gamma R - (\beta_1 E + \beta_2 I_a + \beta_3 I_s)S - \mu S,\\
\frac{dE}{dt} &= (\beta_1 E + \beta_2 I_a + \beta_3 I_s)S - \kappa E - \mu E,\\
\frac{dI_a}{dt} &= \epsilon\kappa E - \omega_a I_a - \mu I_a,\\
\frac{dI_s}{dt} &= (1-\epsilon)\kappa E - \omega_s I_s - \mu I_s,
\end{aligned}$$

TABLE 1. Description of the model's variables and parameters.

Variables/Parameters	Description
$S(t)$	Number of susceptible individuals at a time t
$E(t)$	Number of exposed individuals at a time t
$I_a(t)$	Number of asymptomatically infected individuals at a time t
$I_s(t)$	Number of symptomatically infected individuals at a time t
$Q(t)$	Number of quarantined individuals at a time t
$R(t)$	Number of recovered individuals at a time t
N	Total human population
Λ	Rate of recruitment (from birth and immigration)
μ	Natural death rate and disease-induced death rate
β_1	The transition rate of infection from E class
β_2	The transition rate of infection from I_a class
β_3	The transition rate of infection from I_s class
ϵ	The proportion of E class show no clinical symptoms after the incubation period
κ	Exit rate from E class
ω_a	The recovery rate of individuals in the I_a class
δ	The recovery rate of individuals in the Q class
σ	The proportion of I_s class individuals who have been quarantined
ω_s	Exit rate from I_s class
γ	Rate of reduction of the effect of temporary immunity after the recovery

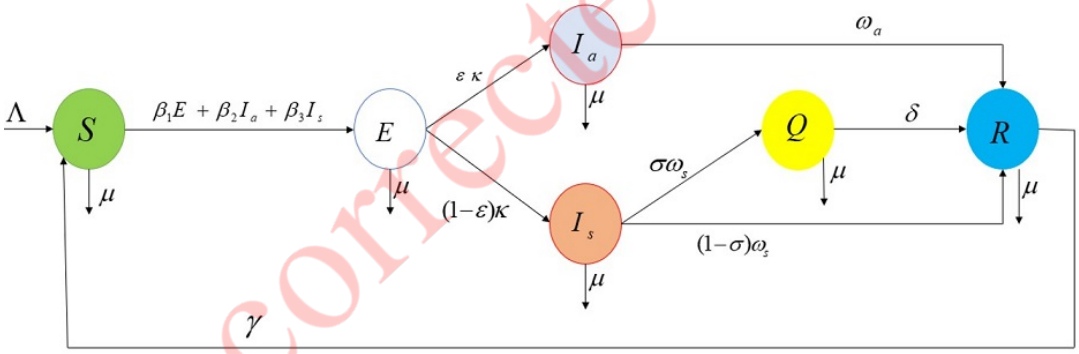

FIGURE 1. Flow chart of SEI_aI_sQRS compartmental model.

$$\begin{aligned}
\frac{dQ}{dt} &= \sigma\omega_s I_s - \delta Q - \mu Q,\\
\frac{dR}{dt} &= \omega_a I_a + (1-\sigma)\omega_s I_s + \delta Q - \gamma R - \mu R.
\end{aligned} \tag{2.2}$$

From the sum of the equations of model Eq. (2.2) we have

$$\frac{dN}{dt} = \Lambda - \mu N. \tag{2.3}$$

Model dynamics can be considered in the region below:

$$\Omega = \Big\{(S, E, I_a, I_s, Q, R) \in \mathbb{R}^6_+ : N \leq \frac{\Lambda}{\mu}\Big\}. \tag{2.4}$$

2.2. **Positivity and boundedness of solutions.**

Theorem 2.1. *Let the initial conditions of the model's variables be given by*

$$\{S(0) \geq 0, E(0) \geq 0, I_a(0) \geq 0, I_s(0) \geq 0, Q(0) \geq 0, R(0) \geq 0 \text{ and } N(0) \geq 0\} \in \Omega.$$

Then the solution set $\{S(t), E(t), I_a(t), I_s(t), Q(t), R(t) \text{ and } N(t)\}$ *is non-negative in* Ω *for all time* $t \geq 0$.

Proof. We use the proof by contradiction to show that the state variable S of the model is positive for all $t \geq 0$. Let that a trajectory crosses the positive cone at time t_1 such that:

$$S(t_1) = 0, \ \frac{dS(t_1)}{dt} \geq 0, \ E(t) > 0, \ I_a(t) > 0,$$

$$I_s(t) > 0, \ Q(t) > 0, \ \text{and } R(t) > 0 \ \text{for all } t \in (0, t_1).$$

Using the first equation of model (2.2), the first assumption results

$$\frac{dS(t_1)}{dt} = \Lambda + \gamma R(t_1) > 0, \tag{2.5}$$

which contradicts the first assumption that $\frac{dS(t_1)}{dt} < 0$. So, $S(t)$ remains positive for all $t \geq 0$.
Using the second equation of model (2.2),

$$\frac{dE(t)}{dt} = \lambda S(t) - (\kappa + \mu)E(t), \tag{2.6}$$

where in above equation $\lambda = \beta_1 E + \beta_2 I_a + \beta_3 I_s$. Since $S(t)$ is non-negative for all $t \geq 0$, we obtain

$$\frac{dE(t)}{dt} \geq -(\kappa + \mu)E(t), \tag{2.7}$$

Solving the above equation results

$$E(t) \geq E(0)\exp(-[\kappa + \mu]t). \tag{2.8}$$

Clearly, $E(t) \geq 0$. Similarly, we can deduce the rest of the dynamic variables of the system remain positive for all $t > 0$ and they are:

$$I_a(t) \geq I_a(0)\exp(-[\omega_a + \mu]t), \tag{2.9}$$

$$I_s(t) \geq I_s(0)\exp(-[\omega_s + \mu]t), \tag{2.10}$$

$$Q(t) \geq Q(0)\exp(-[\delta + \mu]t), \tag{2.11}$$

$$R(t) \geq R(0)\exp(-[\gamma + \mu]t). \tag{2.12}$$

Hence, any solution of the model (2.2) is non-negative for all $t \geq 0$. □

Theorem 2.2. *All positive solutions described in Theorem 2.1 are bounded.*

Proof. As we have seen before $\frac{dN}{dt} = \Lambda - \mu N$, separating the variables and integrating,

$$\begin{aligned}
&\Rightarrow \int \frac{dN}{\Lambda - \mu N} = \int dt,\\
&\Rightarrow -\frac{1}{\mu}\ln(\Lambda - \mu N) = t + c,\\
&\Rightarrow \ln(\Lambda - \mu N) = -\mu t + C, \qquad \text{where } C = -\mu c,\\
&\Rightarrow \Lambda - \mu N = A\exp(-\mu t). \qquad (2.13)
\end{aligned}$$

Which in the Eq. (2.13), $A = \exp(-\mu c)$. It can be written from the (2.13) that

$$N(t) = \frac{1}{\mu}(\Lambda - A\exp(-\mu t)). \qquad (2.14)$$

To get the population size at N_0 we put $t = 0$ in the last equality. So

$$N(0) = \frac{\Lambda}{\mu} - \frac{A}{\mu} = \frac{\Lambda - A}{\mu} = N_0, \qquad (2.15)$$

$$\Rightarrow \quad A = \Lambda - \mu N_0. \qquad (2.16)$$

By replacing (2.16) into (2.14), we get

$$N(t) = \frac{\Lambda}{\mu} - (\frac{\Lambda - \mu N_0}{\mu})\exp(-\mu t). \qquad (2.17)$$

From (2.17), $N(t)$ approaches $\frac{\Lambda}{\mu}$ as $t \to \infty$, therefore, the positive solutions of model (2.2) are bounded. □

3. Mathematical analysis of the model

To obtain the equilibrium points, we put the right-hand side of model (2.2) equal to zero, so we have

$$\begin{aligned}
\Lambda + \gamma R - (\beta_1 E + \beta_2 I_a + \beta_3 I_s)S - \mu S &= 0,\\
(\beta_1 E + \beta_2 I_a + \beta_3 I_s)S - \kappa E - \mu E &= 0,\\
\epsilon\kappa E - \omega_a I_a - \mu I_a &= 0,\\
(1-\epsilon)\kappa E - \omega_s I_s - \mu I_s &= 0,\\
\sigma\omega_s I_s - \delta Q - \mu Q &= 0,\\
\omega_a I_a + (1-\sigma)\omega_s I_s + \delta Q - \gamma R - \mu R &= 0. \qquad (3.1)
\end{aligned}$$

Our model has both disease-free and endemic equilibria which can be determined by (3.1). We denote the disease-free equilibrium point $DFEP$ as

$$\mathbf{X}_{dfep} = (S_{dfep}, E_{dfep}, I_{a\ dfep}, I_{s\ dfep}, Q_{dfep}, R_{dfep}) = \left(\frac{\Lambda}{\mu}, 0, 0, 0, 0, 0\right) = (1, 0, 0, 0, 0, 0).$$

Furthermore, assuming $\lambda^\star = \beta_1 E + \beta_2 I_a + \beta_3 I_s$ then the endemic equilibrium point of (EEP) is denoted by $\mathbf{X}_{eep} = (S^*, E^*, I_a^*, I_s^*, Q^*, R^*)$, that

$$\begin{aligned} S^* &= \frac{\Lambda + \gamma R}{\lambda^\star + \mu}, \\ E^* &= \frac{\lambda^\star S}{\kappa + \mu}, \\ I_a^* &= \frac{\epsilon\kappa E}{\mu + \omega_a}, \\ I_s^* &= \frac{(1-\epsilon)\kappa E}{\mu + \omega_s}, \\ Q^* &= \frac{\sigma\omega_s I_s}{\mu + \delta}, \\ R^* &= \frac{\omega_a I_a + (1-\sigma)\omega_s I_s + \delta Q}{\mu + \gamma}. \end{aligned} \tag{3.2}$$

3.1. **The basic reproduction number of model (2.2).** One of the important factors in the investigation of epidemic diseases is the basic reproduction number $\mathcal{R}_0$. This parameter is an indicator to measure the spread of the pathogen and is the average number of people to whom the infected person can spread the infectious agent. For this aim, we follow the next-generation matrix method [15]. The compartments that directly caused the spread of COVID-19 are from the second, third, and fourth equations of model (2.2). These equations can be written as

$$\frac{dy}{dt} = \Phi(y) - \Psi(y).$$

Where

$$y = (E, I_a, I_s)^T, \Phi(y) = \begin{bmatrix} (\beta_1 E + \beta_2 I_a + \beta_3 I_s) S \\ 0 \\ 0 \end{bmatrix}, \Psi(y) = \begin{bmatrix} (\mu+\kappa)E \\ -\epsilon\kappa E + (\mu + \omega_a) I_a \\ -(1-\epsilon)\kappa E + (\mu + \omega_s) I_s \end{bmatrix},$$

F and V are the jacobian matrices of Φ and Ψ at the $DFEP(\mathbf{X}_{dfep})$ respectively, which are given by

$$F = J(\Phi|\mathbf{X}_{dfep}) = \begin{bmatrix} \beta_1 & \beta_2 & \beta_3 \\ 0 & 0 & 0 \\ 0 & 0 & 0 \end{bmatrix}, V = J(\Psi|\mathbf{X}_{dfep}) = \begin{bmatrix} \mu+\kappa & 0 & 0 \\ -\epsilon\kappa & \mu+\omega_a & 0 \\ -(1-\epsilon)\kappa & 0 & \mu+\omega_s \end{bmatrix},$$

$\mathcal{R}_0$ will be the largest eigenvalue (the spectral radius) of the matrix FV^{-1} , thus

$$\mathcal{R}_0 = \frac{\beta_1}{\kappa+\mu} + \frac{\beta_2\epsilon\kappa}{(\kappa+\mu)(\omega_a+\mu)} + \frac{\beta_3(1-\epsilon)\kappa}{(\kappa+\mu)(\omega_s+\mu)}. \tag{3.3}$$

4. Stability Analysis

We study the global stability of the disease-free equilibrium point using Castilo-Chavez [10]. We rewrite system (2) as

$$\frac{dx}{dt} = F(x, I), \qquad \frac{dI}{dt} = G(x, I), \qquad G(x, 0) = 0.$$

Where $x \in \mathbb{R}$ denotes the number of uninfected $(S(t))$ and $I \in \mathbb{R}^5$ denotes the number of infected individuals $(E(t), I_a(t), I_s(t), Q(t), R(t))$. Let $U_0 = (x^\star, 0)$ be the disease-free equilibrium point of this system, where 0 is a zero vector. The below conditions must be satisfied to guarantee global stability.
(H1): For $\frac{dx}{dt} = F(x, 0), 0$ is globally stable.
(H2): $G(x, I) = AI - \tilde{G}(x, I), \tilde{G}(x, I)$ is non-negative for $(x, I) \in \Omega$,

where $A = D_I G(x^\star, 0)$ is an M-matrix (with off-diagonal elements of A are non-negative) and Ω is the region where the model makes biological sense. In our case

$$U_0 = (x^\star, 0) = (1, 0, 0, 0, 0, 0),$$

and

$$A = \begin{bmatrix} \beta_1 - (\kappa+\mu) & \beta_2 & \beta_3 & 0 & 0 \\ \epsilon\kappa & -(\omega_a+\mu) & 0 & 0 & 0 \\ (1-\epsilon)\kappa & 0 & -(\omega_s+\mu) & 0 & 0 \\ 0 & 0 & \sigma\omega_s & -(\delta+\mu) & 0 \\ 0 & \omega_a & (1-\sigma)\omega_s & \delta & -(\gamma+\mu) \end{bmatrix},$$

that A is an M-matrix. On the other hand

$$G(x, I) = \begin{bmatrix} (\beta_1 E + \beta_2 I_a + \beta_3 I_s)S - (\kappa+\mu)E \\ \epsilon\kappa E - (\omega_a+\mu)I_a \\ (1-\epsilon)\kappa E - (\omega_s+\mu)I_s \\ \sigma\omega_s I_s - (\delta+\mu)Q \\ \omega_a I_a + (1-\sigma)\omega_s I_s + \delta Q - (\gamma+\mu)R \end{bmatrix},$$

and

$$\tilde{G}(x, I) = \begin{bmatrix} (\beta_1 E + \beta_2 I_a + \beta_3 I_s)(1-S) \\ 0 \\ 0 \\ 0 \\ 0 \end{bmatrix},$$

which implies that $\tilde{G}(x, I) \geq 0$ for all $(x, I) \in \Omega$. Therefore, we conclude that the disease-free equilibrium point is globally stable.

Theorem 4.1. *Assuming*

$$G^* = (\beta_1 + \frac{\beta_2\epsilon\kappa}{\mu+\omega_a} + \frac{\beta_3(1-\epsilon)\kappa}{\mu+\omega_s})E^*, \quad b_0 = G^* + \mu,$$
$$b_1 = \kappa + \mu - \beta_1 S^* (\kappa + \mu > \beta_1 S^*), \quad b_2 = \omega_a + \mu, \quad b_3 = \omega_s + \mu,$$
$$b_4 = \delta + \mu, \quad b_5 = \gamma + \mu.$$

then the endemic equilibrium point (X_{eep}) is locally asymptotically stable if the following conditions hold:

$$\mathcal{Q}_0, \mathcal{Q}_1, \mathcal{Q}_2, \mathcal{Q}_3, \mathcal{Q}_4 > 0, \quad \mathcal{Q}_1\mathcal{Q}_2\mathcal{Q}_3 > \mathcal{Q}_3^2 + \mathcal{Q}_1^2\mathcal{Q}_4,$$
$$(\mathcal{Q}_1\mathcal{Q}_4 - \mathcal{Q}_5)(\mathcal{Q}_1\mathcal{Q}_2\mathcal{Q}_3 - \mathcal{Q}_3^2 - \mathcal{Q}_1^2\mathcal{Q}_4) > \mathcal{Q}_5(\mathcal{Q}_1\mathcal{Q}_2 - \mathcal{Q}_3)^2 + \mathcal{Q}_1\mathcal{Q}_5^2.$$

Proof. The Jacobian matrix of (2.2) at the endemic equilibrium point is given by,

$$J(X_{eep}) = \begin{bmatrix} -b_0 & -\beta_1 S^* & -\beta_2 S^* & -\beta_3 S^* & 0 & \gamma \\ G^* & -b_1 & \beta_2 S^* & \beta_3 S^* & 0 & 0 \\ 0 & \epsilon\kappa & -b_2 & 0 & 0 & 0 \\ 0 & (1-\epsilon)\kappa & 0 & -b_3 & 0 & 0 \\ 0 & 0 & 0 & \sigma\omega_s & -b_4 & 0 \\ 0 & 0 & \omega_a & (1-\sigma)\omega_s & \delta & -b_5 \end{bmatrix}.$$

The characteristic polynomial of the Jacobian matrix of the model is given by,

$$\mathcal{P} = (\xi + b_4)(\xi^5 + \mathcal{Q}_4\xi^4 + \mathcal{Q}_3\xi^3 + \mathcal{Q}_2\xi^2 + \mathcal{Q}_1\xi + \mathcal{Q}_0),$$

where

$$\begin{aligned}
\mathcal{Q}_4 &= b_0 + b_1 + b_2 + b_3 + b_5,\\
\mathcal{Q}_3 &= b_2b_5 + b_3b_5 + b_2b_3 + b_0b_5 + b_1b_5 + b_0b_2 + b_0b_3 + b_1b_2 + b_1b_3 + b_0b_1\\
&\quad - \beta_2\epsilon\kappa S^* - \beta_3(1-\epsilon)\kappa S^* + \beta_1 S^* G^*,\\
\mathcal{Q}_2 &= b_2b_3b_5 + b_0b_2b_5 + b_0b_3b_5 + b_1b_2b_5 + b_1b_3b_5 + b_0b_2b_3 + b_1b_2b_3\\
&\quad + b_0b_1b_5 + b_0b_1b_2 + b_0b_1b_3 - \beta_2\epsilon\kappa S^*(b_0 + b_3 + b_5) - \beta_3(1-\epsilon)\kappa S^*(b_0 + b_2 + b_5)\\
&\quad + \beta_1 S^* G^*(b_2 + b_3 + b_5) + \beta_2\epsilon\kappa S^* G^* + \beta_3(1-\epsilon)\kappa S^* G^*,\\
\mathcal{Q}_1 &= b_0b_2b_3b_5 + b_1b_2b_3b_5 + b_0b_1b_2b_5 + b_0b_1b_3b_5 + b_0b_1b_2b_3\\
&\quad - \beta_2\epsilon\kappa S^*(b_0b_5 + b_3b_5) - \beta_2\epsilon\kappa S^* b_0b_3 - \beta_3(1-\epsilon)\kappa S^*(b_0b_5 + b_2b_5)\\
&\quad - \beta_3(1-\epsilon)\kappa S^* b_0b_2 + \beta_1 S^* G^*(b_2b_5 + b_3b_5) + \beta_1 S^* G^* b_2b_3\\
&\quad + \beta_2\epsilon\kappa S^* G^*(b_3 + b_5) + \beta_3(1-\epsilon)\kappa S^* G^*(b_2 + b_5) - \gamma(1-\epsilon)\kappa(1-\sigma)\omega_s G^*,\\
\mathcal{Q}_0 &= b_0b_1b_2b_3b_5 - \beta_2\epsilon\kappa S^* b_0b_3b_5 - \beta_3(1-\epsilon)\kappa S^* b_0b_2b_5 + G^*\beta_1 S^* b_2b_3b_5\\
&\quad + G^*\beta_2 S^*\epsilon\kappa b_3b_5 + G^*\beta_3(1-\epsilon)\kappa S^* b_2b_5 + G^*\gamma\epsilon\kappa\omega_a - \gamma(1-\epsilon)\kappa(1-\sigma)\omega_s G^* b_2.
\end{aligned}$$

It is necessary to note that we assumed $\gamma(1-\epsilon)\kappa G^*(b_2+\xi)\sigma\delta\omega_s = 0$. □

5. Backward bifurcation analysis

In some models, disease does not wipe out simply by reducing $\mathcal{R}_0$ and it is necessary to check whether there is a backward bifurcation or not. Generally, backward bifurcation is a negative concept because the presence of backward bifurcation makes it more difficult to control the disease.

Theorem 5.1. *The model (2.2) shows a backward bifurcation at $\beta_1 = \beta_1^*$ (i.e $\mathcal{R}_0 = 1$) if the parameters satisfy the condition*

$$\kappa + \mu < \frac{\gamma}{\gamma+\mu} M,$$

where

$$M = \frac{\omega_a\epsilon\kappa}{\omega_a+\mu} + \frac{\omega_s\kappa(1-\epsilon)(1-\sigma)}{\omega_s+\mu} + \frac{\delta\sigma\omega_s\kappa(1-\epsilon)}{(\omega_s+\mu)(\delta+\mu)}.$$

Proof. The proof is done using center manifold theory introduced in [9, 11]. Assume

$$X = (x_1, x_2, x_3, x_4, x_5, x_6)^T = (S, E, I_a, I_s, Q, R)^T,$$

and

$$N = x_1 + x_2 + x_3 + x_4 + x_5 + x_6.$$

Then the model (2.2) turns into, $X'(t) = F = (f_1, f_2, f_3, f_4, f_5, f_6)$ that is,

$$\begin{aligned}
f_1 &= \Lambda + \gamma x_6 - (\beta_1 x_2 + \beta_2 x_3 + \beta_3 x_4)x_1 - \mu x_1,\\
f_2 &= (\beta_1 x_2 + \beta_2 x_3 + \beta_3 x_4)x_1 - (\kappa+\mu)x_2,\\
f_3 &= \epsilon\kappa x_2 - (\omega_a+\mu)x_3,\\
f_4 &= (1-\epsilon)\kappa x_2 - (\omega_s+\mu)x_4,\\
f_5 &= \sigma\omega_s x_4 - (\delta+\mu)x_5,\\
f_6 &= \omega_a x_3 + (1-\sigma)\omega_s x_4 + \delta x_5 - (\gamma+\mu)x_6.
\end{aligned} \tag{5.1}$$

Note that β_1 has been chosen as a bifurcation parameter and β_1^* is its critical value and setting $\mathcal{R}_0 = 1$, we obtain $\beta_1^* T_1 + T_3 = 1$ or $\beta_1 = \beta_1^* = \frac{1-T_3}{T_1}$. Where

$$T_1 = \frac{1}{\kappa+\mu}, \quad T_2 = \frac{\beta_2\epsilon\kappa}{\omega_a+\mu} + \frac{\beta_3(1-\epsilon)\kappa}{\omega_s+\mu}, \quad T_3 = T_2T_1.$$

The Jacobian of the system (5.1) at the disease-free equilibrium point (X_{dfep}) with β_1^* is given by,

$$J(X_{dfep}) = \begin{bmatrix} -\mu & -\beta_1^* & -\beta_2 & -\beta_3 & 0 & \gamma \\ 0 & -(\kappa+\mu-\beta_1^*) & \beta_2 & \beta_3 & 0 & 0 \\ 0 & \epsilon\kappa & -(\omega_a+\mu) & 0 & 0 & 0 \\ 0 & (1-\epsilon)\kappa & 0 & -(\omega_s+\mu) & 0 & 0 \\ 0 & 0 & 0 & \sigma\omega_s & -(\delta+\mu) & 0 \\ 0 & 0 & \omega_a & (1-\sigma)\omega_s & \delta & -(\gamma+\mu) \end{bmatrix}.$$

The Jacobian matrix above has a single zero eigenvalue with all the other eigenvalues having negative real parts. Hence, based on the center manifold theory approach given by Theorem 3.2 of Castillo-Chavez and Song [11] we can analyze the system of Equations (5.1).
Let the right-eigenvector of the Jacobian matrix $J(X_{dfep})$ be in the form of $W = (w_1, w_2, w_3, w_4, w_5, w_6)^T$, thus

$$\begin{aligned} -\mu w_1 - \beta_1^* w_2 - \beta_2 w_3 - \beta_3 w_4 + \gamma w_6 &= 0, \\ -(\kappa+\mu-\beta_1^*)w_2 + \beta_2 w_3 + \beta_3 w_4 &= 0, \\ \epsilon\kappa w_2 - (\omega_a+\mu)w_3 &= 0, \\ (1-\epsilon)\kappa w_2 - (\omega_s+\mu)w_4 &= 0, \\ \sigma\omega_s w_4 - (\delta+\mu)w_5 &= 0, \\ \omega_a w_3 + (1-\sigma)\omega_s w_4 + \delta w_5 - (\gamma+\mu)w_6 &= 0. \end{aligned}$$

From the above, it is easy to find that w_1 through w_6 in terms of w_2. Thus

$$\begin{aligned} w_1 &= \frac{1}{\mu}\Big(-(\kappa+\mu)\frac{\gamma}{\gamma+\mu}M\Big)w_2, \\ w_2 &= w_2 > 0, \\ w_3 &= \frac{\epsilon\kappa}{\omega_a+\mu}w_2, \\ w_4 &= \frac{(1-\epsilon)\kappa}{\omega_s+\mu}w_2, \\ w_5 &= \frac{\sigma\omega_s(1-\epsilon)\kappa}{(\omega_s+\mu)(\delta+\mu)}w_2, \\ w_6 &= \frac{1}{\gamma+\mu}Mw_2. \end{aligned}$$

Similarly, the left-eigenvector of $J(X_{dfep})$ is considered as $V = (v_1, v_2, v_3, v_4, v_5, v_6)$ satisfies the following set of equations:

$$\begin{aligned} -\mu v_1 &= 0, \\ -\beta_1^* v_1 - (\kappa+\mu-\beta_1^*)v_2 + \epsilon\kappa v_3 + (1-\epsilon)\kappa v_4 &= 0, \\ -\beta_2 v_1 + \beta_2 v_2 - (\omega_a+\mu)v_3 + \omega_a v_6 &= 0, \\ -\beta_3 v_1 + \beta_3 v_2 - (\omega_s+\mu)v_4 + \sigma\omega_s v_5 + (1-\sigma)\omega_s v_6 &= 0, \\ -(\delta+\mu)v_5 + \delta v_6 &= 0, \\ \gamma v_1 - (\gamma+\mu)v_6 &= 0. \end{aligned} \tag{5.2}$$

Then solving Equation (5.2), we get

$$v_1 = v_5 = v_6 = 0, \quad v_3 = \frac{\beta_2 v_2}{\omega_a + \mu}, \quad v_4 = \frac{\beta_3 v_2}{\omega_s + \mu}, \quad v_2 = v_2 > 0.$$

If

$$v_2 w_2 = \left(1 + \frac{\beta_2 \epsilon \kappa}{(\omega_a + \mu)^2} + \frac{\beta_3 (1-\epsilon)\kappa}{(\omega_s + \mu)^2}\right)^{-1} > 0,$$

then the left-eigenvector and right-eigenvector satisfy in the condition of

$$V.W = 1.$$

The first bifurcation coefficient at X_{dfep} is as follows:

$$\begin{aligned}\mathbf{a} &= \sum_{k,i,j=1}^{6} v_k w_i w_j \frac{\partial^2 f_k}{\partial x_i \partial x_j}(X_{dfep}, \beta_1^*) \\ &= \sum_{i,j=1}^{6} \left[v_2 w_i w_j \frac{\partial^2 f_2}{\partial x_i \partial x_j}(X_{dfep}, \beta_1^*) + v_3 w_i w_j \frac{\partial^2 f_3}{\partial x_i \partial x_j}(X_{dfep}, \beta_1^*) + v_4 w_i w_j \frac{\partial^2 f_4}{\partial x_i \partial x_j}(X_{dfep}, \beta_1^*) \right]. \end{aligned} \tag{5.3}$$

Algebraic calculations show that

$$\begin{aligned} &\frac{\partial^2 f_2}{\partial x_1 \partial x_2}(X_{dfep}, \beta_1^*) = \beta_1^*, \quad \frac{\partial^2 f_2}{\partial x_1 \partial x_3}(X_{dfep}, \beta_1^*) = \beta_2, \\ &\frac{\partial^2 f_2}{\partial x_1 \partial x_4}(X_{dfep}, \beta_1^*) = \beta_3, \quad \frac{\partial^2 f_2}{\partial x_2 \partial x_1}(X_{dfep}, \beta_1^*) = \beta_1^*, \\ &\frac{\partial^2 f_2}{\partial x_3 \partial x_1}(X_{dfep}, \beta_1^*) = \beta_2, \quad \frac{\partial^2 f_2}{\partial x_4 \partial x_1}(X_{dfep}, \beta_1^*) = \beta_3. \end{aligned} \tag{5.4}$$

The rest of the second derivatives for $\mathbf{a}$ in (5.3), then $\mathbf{a}$ is given by

$$\mathbf{a} = \frac{2v_2}{\mu}\left(-(\kappa + \mu) + \frac{\gamma}{\gamma + \mu} M \right) \left[\beta_1^* + \frac{\epsilon \kappa \beta_2}{\omega_a + \mu} + \frac{(1-\epsilon)\kappa \beta_3}{\omega_s + \mu} \right] w_2^2.$$

Since

$$\beta_1^* + \frac{\epsilon \kappa \beta_2}{\omega_a + \mu} + \frac{(1-\epsilon)\kappa \beta_3}{\omega_s + \mu},$$

is always positive, then the bifurcation coefficient $\mathbf{a}$ can be positive if

$$-(\kappa + \mu) + \frac{\gamma}{\gamma + \mu} M > 0.$$

On the other hand, the second bifurcation coefficient at X_{dfep} and bifurcation parameter β_1^* is given by,

$$\begin{aligned}\mathbf{b} &= \sum_{k,j=1}^{6} v_k w_j \frac{\partial^2 f_k}{\partial x_j \partial \beta_1^*}(X_{dfep}, \beta_1^*) \\ &= \sum_{j=1}^{6} \left[v_2 w_j \frac{\partial^2 f_2}{\partial x_j \partial \beta_1^*}(X_{dfep}, \beta_1^*) + v_3 w_j \frac{\partial^2 f_3}{\partial x_j \partial \beta_1^*}(X_{dfep}, \beta_1^*) + v_4 w_j \frac{\partial^2 f_4}{\partial x_j \partial \beta_1^*}(X_{dfep}, \beta_1^*) \right] = v_2 w_2. \end{aligned}$$

Clearly, $b > 0$. In addition, if we set $M = 0$ then $\mathbf{a}$ will be negative which means the model (5.1) will not undergo a backward bifurcation at $\mathcal{R}_0 = 1$. □

6. Sensitivity index and numerical analysis

Sensitivity analysis reveals the influence of the model parameters, which have the most significant impact on the basic reproduction number of the COVID-19 model system. It is derivable to the parameter α, the normalized forward sensitivity index of basic reproduction number $\mathcal{R}_0$ is denoted by $\Upsilon_{\alpha}^{\mathcal{R}_0} = \frac{\partial \mathcal{R}_0}{\partial \alpha} \times \frac{\alpha}{\mathcal{R}_0}$
We repeated the above formula for each of the parameters on which the basic generating number depended and we will have the following relations:

$$\Upsilon_{\beta_1}^{\mathcal{R}_0} = \frac{\beta_1(\omega_a+\mu)(\omega_s+\mu)}{\beta_1(\omega_a+\mu)(\omega_s+\mu)+\beta_2\epsilon\kappa(\omega_s+\mu)+\beta_3(1-\epsilon)\kappa(\omega_a+\mu)} > 0,$$

$$\Upsilon_{\beta_2}^{\mathcal{R}_0} = \frac{\beta_2\epsilon\kappa(\omega_s+\mu)}{\beta_1(\omega_a+\mu)(\omega_s+\mu)+\beta_2\epsilon\kappa(\omega_s+\mu)+\beta_3(1-\epsilon)\kappa(\omega_a+\mu)} > 0,$$

$$\Upsilon_{\beta_3}^{\mathcal{R}_0} = \frac{\beta_3(1-\epsilon)\kappa(\omega_a+\mu)}{\beta_1(\omega_a+\mu)(\omega_s+\mu)+\beta_2\epsilon\kappa(\omega_s+\mu)+\beta_3(1-\epsilon)\kappa(\omega_a+\mu)} > 0,$$

$$\Upsilon_{\kappa}^{\mathcal{R}_0} = \frac{-\beta_1\kappa(\omega_a+\mu)(\omega_s+\mu)+\beta_2\epsilon\kappa^2(\omega_s+\mu)+\beta_3(1-\epsilon)\kappa^2(\omega_a+\mu)}{(\kappa+\mu)[\beta_1(\omega_a+\mu)(\omega_s+\mu)+\beta_2\epsilon\kappa(\omega_s+\mu)+\beta_3(1-\epsilon)\kappa(\omega_a+\mu)]},$$

$$\Upsilon_{\epsilon}^{\mathcal{R}_0} = \frac{\beta_2\epsilon\kappa(\omega_s+\mu)-\beta_3\epsilon\kappa(\omega_a+\mu)}{\beta_1(\omega_a+\mu)(\omega_s+\mu)+\beta_2\epsilon\kappa(\omega_s+\mu)+\beta_3(1-\epsilon)\kappa(\omega_a+\mu)},$$

$$\Upsilon_{\omega_a}^{\mathcal{R}_0} = \frac{-\beta_2\epsilon\kappa\omega_a(\omega_s+\mu)}{(\omega_a+\mu)[\beta_1(\omega_a+\mu)(\omega_s+\mu)+\beta_2\epsilon\kappa(\omega_s+\mu)+\beta_3(1-\epsilon)\kappa(\omega_a+\mu)]} < 0,$$

$$\Upsilon_{\omega_s}^{\mathcal{R}_0} = \frac{-\beta_3(1-\epsilon)\kappa\omega_s(\omega_a+\mu)}{(\omega_s+\mu)[\beta_1(\omega_a+\mu)(\omega_s+\mu)+\beta_2\epsilon\kappa(\omega_s+\mu)+\beta_3(1-\epsilon)\kappa(\omega_a+\mu)]} < 0,$$

$$\Upsilon_{\mu}^{\mathcal{R}_0} = \frac{-\mu[\beta_1(\omega_a+\mu)^2(\omega_s+\mu)^2+\beta_2\epsilon\kappa(2\mu+\kappa+\omega_a)(\omega_s+\mu)^2+\beta_3(1-\epsilon)\kappa(2\mu+\kappa+\omega_s)(\omega_a+\mu)^2]}{(\kappa+\mu)(\omega_a+\mu)(\omega_s+\mu)[\beta_1(\omega_a+\mu)(\omega_s+\mu)+\beta_2\epsilon\kappa(\omega_s+\mu)+\beta_3(1-\epsilon)\kappa(\omega_a+\mu)]} < 0.$$

Therefore, according to the obtained results, it can be written in summary form:

$$\Upsilon_{p}^{\mathcal{R}_0} > 0 \qquad for \quad p = \beta_1, \beta_2, \beta_3,$$
$$\Upsilon_{q}^{\mathcal{R}_0} < 0 \qquad for \quad q = \omega_a, \omega_s, \mu,$$

Also, it is not possible to give a definite opinion about $\Upsilon_{\epsilon}^{\mathcal{R}_0}$ and $\Upsilon_{\kappa}^{\mathcal{R}_0}$ because their sign depends on the values of the parameters.
Therefore, with the increase of β_1, β_2 and β_3 parameters, the basic reproduction number $\mathcal{R}_0$ also increases, while with the increase of ω_a, ω_s and μ the basic reproduction number decreases. Numerical results for our model were performed using the parameter values in Table 2. All parameters are assumed. Simulation for the model (2.2) is done using Matlab $R2016b$ encoded with an $ODE45$ solver, with an initial population of $S(0) = 23$, $E(0) = 18$, $I_a(0) = 19$, $I_s(0) = 39$, $Q(0) = 5$, $R(0) = 38$. Figure 2 shows when the proportion of symptomatically infected class individuals who have been quarantined (σ) increases, the population of recovered (R) and quarantined (Q) compartments increases, and the population of asymptomatically infected (I_a), symptomatically infected (I_s) and exposed (E) classes

TABLE 2. Model parameter values.

Parameter	Value
Λ	0.35
β_1	0.005
β_2	0.01
β_3	0.2
ϵ	0.7
κ	0.4
δ	0.05
ω_a	0.03
σ	0.6
ω_s	0.08
γ	0.001
μ	0.000036

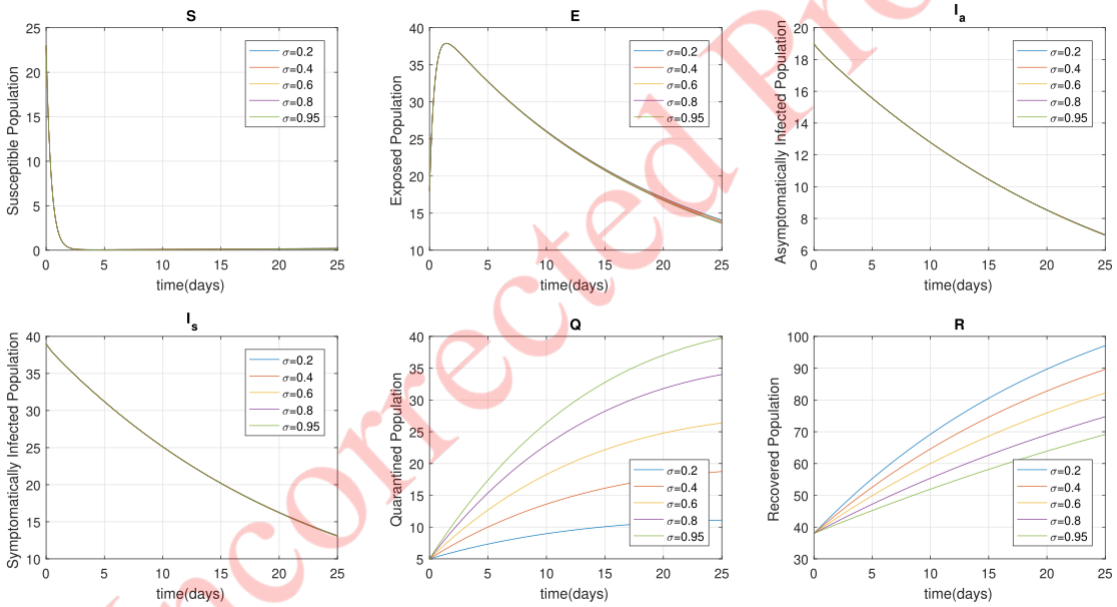

FIGURE 2. Solution curves depicting the impact of the proportion of symptomatically infected class individuals who have been quarantined (σ) on all of the compartments of the model (2.2).

decreases. It implies that quarantine helps to limit the spread of COVID-19.

It can be seen in Figure 3, as the recovery rate of individuals in the quarantined class (δ) increases, the population of S, E, I_a and I_s compartments decreases, and the population of Q and R compartments increases. As displayed in Figure 4, over time, recovered individuals lose their immunity against the disease thus increasing the amount of rate of reduction of the effect of temporary immunity after the recovery (γ) added to the number of exposed (E), infected (I_a and I_s) and quarantined (Q) individuals. It implies that the reversibility of the disease causes the disease to spread again and thus impose a cost on the economy of the countries. Figure 5 shows that when the recovery rate of individuals in the asymptomatically infected class (ω_a) is increasing, the population of recovered individuals (R)

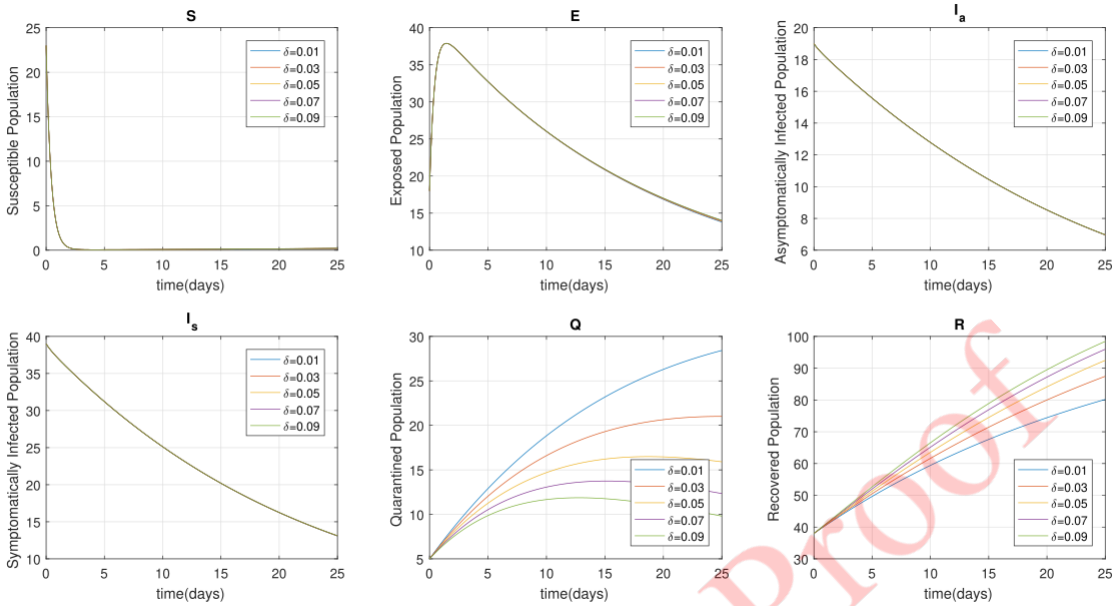

FIGURE 3. Solution curves depicting the impact of the recovery rate of individuals in the quarantined class (δ) on all of the compartments of the model (2.2).

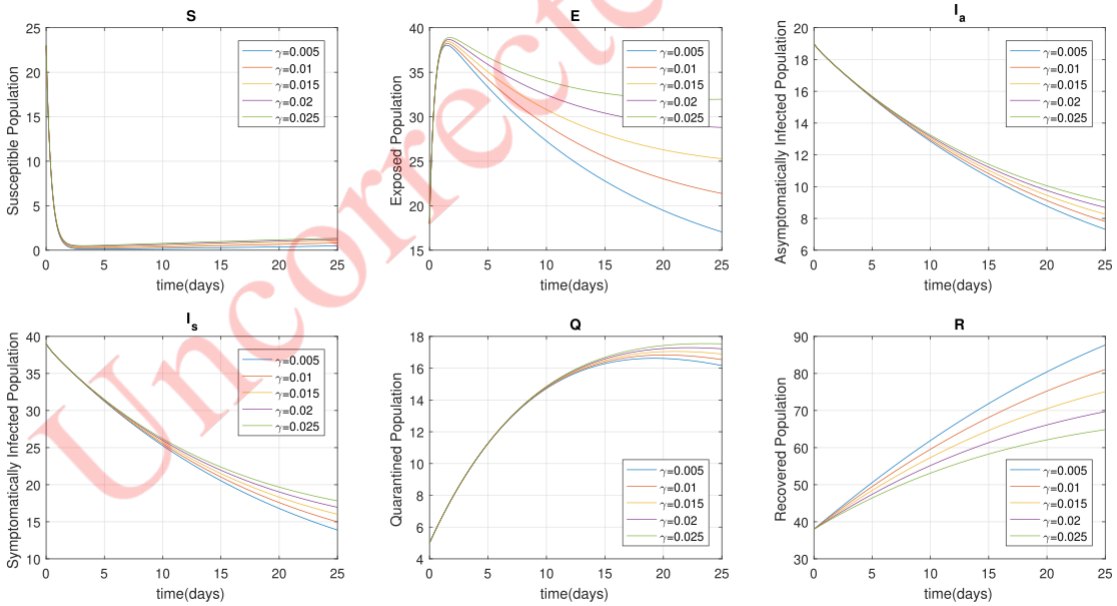

FIGURE 4. Solution curves depicting the impact of rate of reduction of the effect of temporary immunity after the recovery (γ) on all of the compartments of the model (2.2).

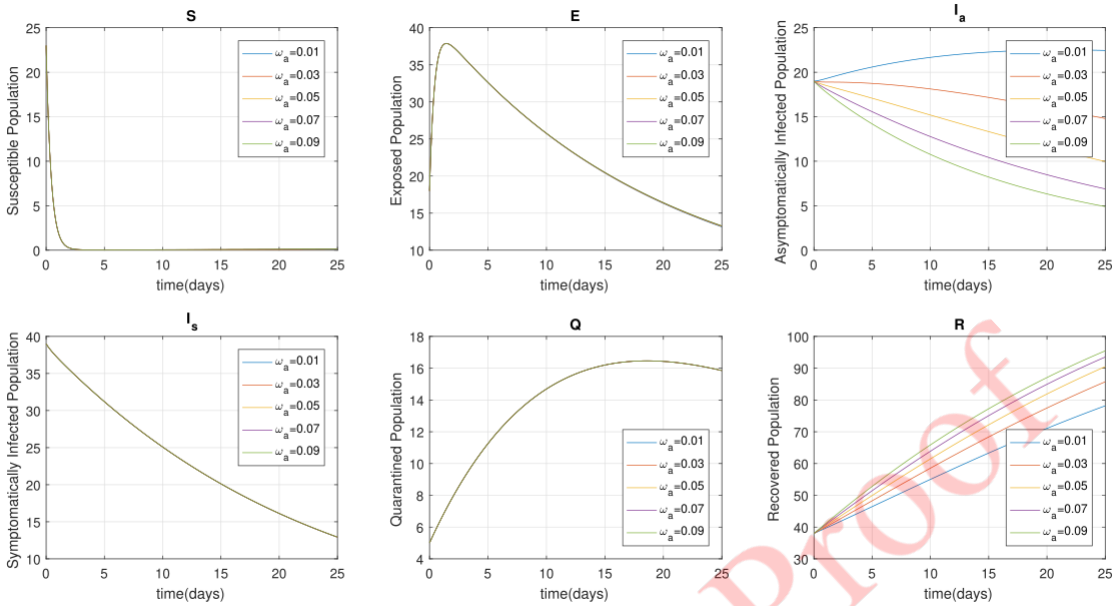

FIGURE 5. Solution curves depicting the impact of the recovery rate of asymptomatically infected individuals class (ω_a) on all of the compartments of the model (2.2).

increases and the population of asymptomatically infected individuals (I_a) decreases. It can be seen in Figure 6, that

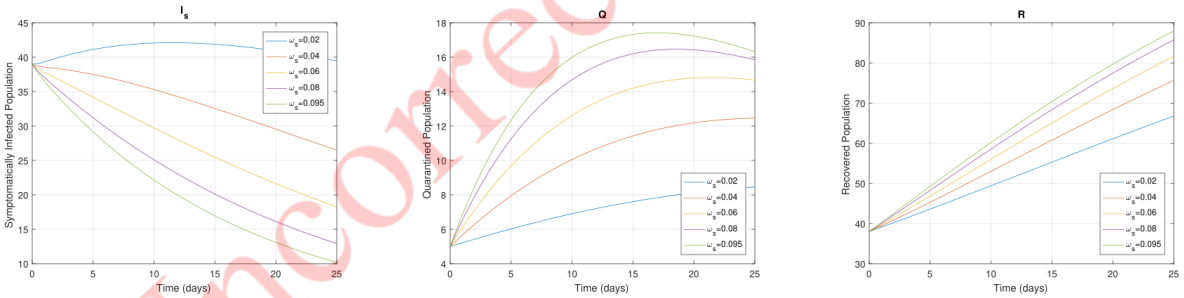

FIGURE 6. Solution curves depicting the impact of the exit rate from symptomatically infected class (ω_s) on symptomatically infected (I_s), quarantined (Q) and recovered (R) compartments of the model (2.2).

when the exit rate from the symptomatically infected class (ω_s) increases, the population of quarantined (Q) and recovered (R) compartments increases.

7. Conclusion

In this paper, we consider a mathematical model comprised of six compartments as, susceptible (S), exposed (E), symptomatically infected (I_s), asymptomatically infected (I_a), quarantined (Q), and recovered (R). We proved the boundedness of model solutions and obtained both the disease-free equilibrium point and the endemic equilibrium

point for our model. By using the next-generation matrix method, we calculated the basic reproduction number $\mathcal{R}_0$. We proved our model at the disease-free equilibrium point is globally stable and at the endemic equilibrium point is locally asymptotically stable. We applied the center manifold theorem to analyze backward bifurcation. After that, we briefly discussed sensitivity analysis and numerical simulations also confirmed that quarantine helps to limit the COVID-19 virus.

Funding

This research did not receive any specific grant from the funding agencies in the public, commercial, or not-for-profit sectors.

Declarations

Conflicts of interest None.

References

[1] A. Ahmed, B. Salam, M. Mohammad, A. Akgul, and S. H. Khoshnaw, *Analysis coronavirus disease (COVID-19) model using numerical approaches and logistic model*, Aims Bioeng., *7*(3) (2020), 130146.
[2] *AIDS epidemic update: December 2006*, [Accessed 2006 December 15]; Available from: https://data.unaids.org/pub/epireport/2006/2006_epiupdate_en.pdf.
[3] A. Akgl, N. Ahmed, A. Raza, Z. Iqbal, M. Rafiq, D. Baleanu, and M. A. U. Rehman, *New applications related to Covid-19*, Res. Phys., *20* (2021), 103663.
[4] P. N. A. Akuka, B. Seidu, and C. S. Bornaa, *Mathematical analysis of COVID-19 transmission dynamics model in Ghana with double-dose vaccination and quarantine*, Computational and mathematical methods in medicine, 2022.
[5] A. D. Algarni, A. B. Hamed, M. Hamdi, H. Elmannai, and S. Meshoul, *Mathematical COVID-19 model with vaccination: a case study in Saudi Arabia*, PeerJ Comput. Sci., *8* (2022), e959.
[6] R. M. Anderson and R. M. May, *Infectious diseases of humans: dynamics and control*, Oxford University Press, 1992.
[7] N. T. J. Bailey, *The mathematical theory of infectious diseases and its applications*, 2nd ed. Scotland: Richard Griffin and Company, 1975.
[8] C. Baishya, R. N. Premakumari, M. E. Samei, and M. K. Naik, *Chaos control of fractional order nonlinear bloch equation by utilizing sliding mode controller*, Chaos, Solitons and Fractals, *174* (2023), 113773.
[9] J. Carr, *Applications Centre Manifold Theory*, Springer-Verlog, New York, 1981.
[10] C. C. Chavez, Z. Feng, and W. Huang, *On the computation of R_0 and its role in global stability*, IMA Volumes in Mathematics and Its Applications, *125* (2002), 229250.
[11] C. C. Chavez and B. Song, *Dynamical models of tuberculosis and their application*, Math Biosci Eng, (2004), 361-404.
[12] G. B. Chapman, M. Li, J. Vietri, Y. Ibuka, D. Thomas, H. Yoon, and A. P. Galvani, *Using game theory to examine incentives in influenza vaccination behavior*, Psychological science, *23*(9) (2012), 1008-1015.
[13] A. N. Chatterjee and F. Al Basir, *A model for SARS-CoV-2 infection with treatment*, Computational and mathematical methods in medicine, 2020.
[14] M. Das, G. Samanta, and M. D. L. Sen, *A fractional order model to study the effectiveness of government measures and public behaviours in COVID-19 pandemic*, Mathematics, 2022.
[15] P. V. Driessche and J. Watmough, *Reproduction numbers and sub-threshold endemic equilibria for compartmental models of disease transmission*, Mathematical bioscience, *180* (2002), 29-48.
[16] M. Farman, A. Akgl, A. Ahmad, D. Baleanu, and M. U. Saleem, *Dynamical transmission of coronavirus model with analysis and simulation*, CMES[1] Computer Modeling in Engineering and Sciences, (2021), 753769.
[17] M. Farman, A. Aqeel, A. Akgl, M. U. Saleem, M. Naeem, and D. Baleanu, *Epidemiological analysis of the coronavirus disease outbreak with random effects*, Computers, Materials, Continua, (2021), 32153227.

[18] F. Fenner, D. Henderson, I. Arita , Z. Jezek, and I. Ladnyi, *Smallpox vaccine and vaccination in the intensified smallpox eradication programme*, Geneva: World Health Organization, (1988), 539-592.
[19] R. Ghostine, M. Gharamti, S. Hassrouny, and I. Hoteit, *An extended SEIR model with vaccination for forecasting the COVID-19 pandemic in Saudi Arabia using an ensemble Kalman filter*, Mathematics, 2021.
[20] K. E. Hail, M. Khalid, and A. Ouhinou, *Early-confinement strategy to tackling COVID-19 in Morocco; a mathematical modelling study*, RAIRO-Oper. Res., *56* (2022), 4023-4033.
[21] A. W. Hickman, R. J. Jaramillo, J. F. Lechner, and N. F. Johnson, α *-Particle induced p53 protein expression in a rat lung epithelial cell strain*, Cancer Res, *54*(22) (1994), 5797-5800.
[22] M. Houas and M. E. Samei, *Existence and stability of solutions for linear and nonlinear Damping of q-fractional Duffing-Rayleigh problem*, Mediterranean Journal of Mathematics, 2023.
[23] N. F. Johnson, N. Velasquez, N. J. Restrepo, R. Leahy, N. Gabriel, S. E. Oud, M. Zheng, P. Manrique, S. Wuchty, and Y. Lupu, *The online competition between pro- and anti- vaccination views*, Nature, *582* (2020), 230-233.
[24] T. Kherraz, M. Benbachir, M. Lakrib, M. E. Samei, M. K. A. Kaabar, and S. A. Bhanotar, *Existance and uniqueness results for a fractional boundary value problems with multiple orders of fractional derivatives and integrals*, SSRN Electronic Journal, 2023.
[25] B. Mohammadaliee, V. Roomi, and M. E. Samei, *SEIARS model for analyzing COVID-19 pandemic process via ψ-Caputo fractional derivative and numerical simulation*, Scientific Reports, 2024.
[26] A. Pandey, M. C. Fitzpatrick, S. M. Moghadas, T. N. Vilches, C. Ko, A. Vasan, and A. P. Galvani, *Modelling the impact of a high-uptake bivalent booster scenario on the COVID-19 burden and health care costs in New York City*, The Lancet Regional Health-Americas, 2023.
[27] M. Parsamanesh and M. Erfanian, *Global dynamics of an epidemic model with standard incidence rate and vaccination strategy*, Chaos, Solitons and Fractals , *117* (2018), 192199.
[28] M. Parsamanesh and M. Erfanian, *Stability and bifurcations in a discretetime epidemic model with vaccination and vital dynamics*, BMC Bioinformatics, 2020.
[29] M. Parsamanesh and M. Erfanian, *Stability and bifurcations in a discrete-time SIVS model with saturated incidence rate*, Chaos, Solitons and Fractals, *150* (2021), 111178.
[30] M. Parsamanesh and M. Erfanian, *Global dynamics of a mathematical model for propagation of infection diseases with saturated incidence rate*, Journal of Advanced Mathematical Modeling, 2021.
[31] J. S. Peiris, K. Y. Yuen, A. D. Osterhaus, and K. Sthr, *The severe acute respiratory syndrome*, The New England Journal of Medicine, *349*(25) (2003), 2431-2441.
[32] A. Remuzzi and G. Remuzzi, *COVID-19 and Italy: what next*, Lancet (London, England), 2020.
[33] S. Rezapour, H. Mohammadi, and M. E. Samei, *SEIR epidemic model for COVID-19 transmission by Caputo derivative of fractional order*, Advances in Difference Equations, 2020.
[34] S. W. Teklu, *Mathematical analysis of the transmission dynamics of COVID-19 infection in the presence of intervention strategies*, Journal of biological dynamics, *16*(1) (2022), 640-664.
[35] A. Zangrillo, L. Beretta, P. Silvani, S. Colombo, A. M. Scandroglio, and A. Dell'Acqua, et al, *Fast reshaping of intensive care unit facilities in a large metropolitan hospital in Milan, Italy: facing the COVID-19 pandemic emergency. Critical care and resuscitation*, journal of the Australasian Academy of Critical care Medicine, *22*(2) (2020), 91-94.
[36] H. Zhu, L. Wei, and P. Niu, *The novel coronavirus outbreak in Wuhan, China*, Global health research and policy, 2020.